

Neoadjuvant PD-1 blockade plus chemotherapy induces a high pathological complete response rate and anti-tumor immune subsets in clinical stage III gastric cancer

Xiaohuan Tang^a, Mengyuan Li^b, Xiaolong Wu^a, Ting Guo^a, Li Zhang^c, Lei Tang^d, Fangzhou Jia^e, Ying Hu^e, Yan Zhang^a, Xiaofang Xing^a, Fei Shan^a, Xiangyu Gao^a, and Ziyu Li^a

^aKey Laboratory of Carcinogenesis and Translational Research (Ministry of Education), Department of Gastrointestinal Cancer Center, Ward I, Peking University Cancer Hospital & Institute, Beijing, P.R. China; ^bDepartment of Radiation Oncology, Peking University 3rd Hospital, Beijing, P.R. China; ^cDepartment of Pathology, Peking University Cancer Hospital & Institute, Beijing, P.R. China; ^dDepartment of Radiology, Peking University Cancer Hospital & Institute, Beijing, P.R. China; ^eBiological Sample Bank, Peking University Cancer Hospital & Institute, Beijing, P.R. China

ABSTRACT

First-line PD-1 blockade plus chemotherapy significantly improves the survival benefits in late-stage gastric cancer (GC) patients. However, the pathological response rate and effects on the immune microenvironment of neoadjuvant PD-1 blockade plus chemotherapy in patients with cTNM-stage III GC remain to be elucidated. Patients with cTNM-stage III GC who underwent neoadjuvant PD-1 blockade plus chemotherapy and surgery were enrolled. Four *in vivo* models bearing GC were jointly established to investigate the specific roles of chemotherapy and PD-1 blockade for GC treatment. The tumor immune microenvironment was analyzed by hematoxylin and eosin (H&E) and IHC staining, multicolor flow cytometry and immunofluorescence. A total of 75 patients with cTNM-stage III (cT2-4N1-3M0) gastric cancer who received neoadjuvant PD-1 blockade plus chemotherapy (SOX/XELOX) were included in this study. After treatment, 21 (28.0%) and 57 (76.0%) patients achieved pathological complete response (pCR) and post-therapy pathological downstaging. Subgroup analyses revealed that patients with CPS >1 (32.6% vs 8.3%) and dMMR (35.7% vs 25.4%) subtype had better efficacy. Additionally, the resected specimens showed more anti-tumor immune infiltration indicating a response to neoadjuvant PD-1 blockade plus chemotherapy. Multicolor immunofluorescence and *in vivo* experiments on mouse models revealed that elevated M1/M2 ratio of macrophages, CD8 + T cells and plasma cells indicated effective response to treatment. Furthermore, neoadjuvant PD-1 blockade plus chemotherapy neither delayed surgery nor increased postoperative complication rate. The analyses indicate neoadjuvant PD-1 blockade plus chemotherapy is a promising therapeutic strategy in patients with cTNM-stage III GC with an encouraging pCR rate.

ARTICLE HISTORY

Received 31 August 2022
Revised 10 October 2022
Accepted 10 Octo 2022

KEYWORDS

cTNM-stage III gastric cancer; neoadjuvant PD-1 blockade plus chemotherapy; pathological complete response; tumor microenvironment; immune cell subpopulations

Background

Gastric cancer (GC) is the fifth most common malignancy and fourth most common death caused by cancers.¹ The currently standard management for resectable advanced GC (AGC, cTNM-stage II–III) is perioperative chemotherapy and gastrectomy plus lymph node resection.^{2–4} Although the survival benefits of neoadjuvant chemotherapy for patients with resectable AGC have been verified by multiple clinical trials,^{2,5,6} a significant proportion of patients is insensitive to NACT and the pathological complete response (pCR) rate, a promising surrogate for survival, remains low ranging from 4.6% to 10%.^{7,8} Therefore, developing novel therapeutic strategies to increase the pCR rate for neoadjuvant therapy is a significant clinical issue for the current treatment of patients with AGC.

Antibodies against PD-1 have increasingly drawn the attention of researchers from different disciplines due to their remarkable efficacy.^{9,10} Substantial academic and clinical studies revealed that PD-1 antibodies significantly inhibit tumor

growth by activating anti-tumor immune cells in various cancer types. Furthermore, the therapeutic efficacy of PD-1 blockade was found to be better when administered preoperatively.⁹ The recent clinical trials suggest that neoadjuvant treatment with PD-1 inhibitors achieved 15.0%–34.6% pCR rates in melanoma,¹¹ colon cancer,¹² and lung cancer,¹³ higher than those induced by previous traditional strategies. We noticed that in several recent studies, administration of PD-1 blockades in GC patients also achieved an encouraging efficacy,^{14–17} but without neoadjuvant data. Furthermore, a recent study showed that first-line PD-1 blockade plus chemotherapy significantly prolonged the survival of GC patients, compared with chemotherapy alone.¹⁸ However, the roles and mechanisms of PD-1 blockade plus chemotherapy in the neoadjuvant therapy of AGC patients remain further investigated.

Precious studies concluded that AGC patients with stage III benefit more from neoadjuvant chemotherapy than stage II.¹⁹ Besides, previous clinical studies revealed that the combined positive score (CPS) of PD-L1 is associated with response to

PD-1 blockade.²⁰ In addition, studies also found that the levels of microsatellite instability (MSI)/mismatch repair (MMR) and tumor mutation burden (TMB) may be effective markers to screen potential benefit patients for immunotherapy.^{20,21} However, the optimal marker to screen AGC patients who are sensitive to PD-1 blockade plus chemotherapy is still not clear.

Tumor microenvironment (TME) has been proven to be an integral part of the tumor and significantly influences tumor progression and therapeutic outcomes.²² Despite the current clinical success of PD-1 blockade, its effects on tumor TME remain to be further elucidated. The advances in single-cell technology and multi-color flow cytometry allow us to identify the dynamic characterization of tumor-infiltrating immune cells and functional subpopulations in the TME.²³ For example, a recent single-cell study found that the phenotypes of T lymphocytes in TME are associated with tumor development and often remain an exhausted state.²⁴ Thus, switching exhausted T cells into effector antitumor T lymphocytes may be an important issue for cancer treatment. In addition, nature killing (NK)-cell and M1-macrophage contribute to kill tumor cells during chemotherapy.²⁵ Understanding the dynamic alterations of immune cells in TME during PD-1 blockade or chemotherapy in AGC patients is important to identify effector cells and therapeutic biomarkers. Therefore, we have designed and performed this study to investigate the pathological response of neoadjuvant PD-1 blockade plus chemotherapy in stage III GC patients, and explore the impacts on dynamic changes in the TME.

Methods

Patients and study design

Seventy-five patients with stage III GC who received neoadjuvant PD-1 blockade plus chemotherapy were enrolled in the study. The regimens of neoadjuvant chemotherapy were 5-fluorouracil-based, mainly including SOX and XELOX; while the PD-1 blockade was achieved by PD-1 antibodies, mainly including Pembrolizumab and Nivolumab. All enrolled patients were diagnosed and clinically staged with endoscopic biopsy specimen analysis by two pathologists, and contrast-enhanced computed tomography (CT). All patients underwent neoadjuvant PD-1 blockade plus chemotherapy and D2 gastrectomy plus lymphadenectomy at the Peking University Cancer Hospital (PKUCH), between June 2017 and May 2022. Primary tumors and lymph nodes were deemed to be surgically resectable according to the surgeon's evaluation. The pathological stage was evaluated, and tumors were graded according to the 8th edition of the tumor-node-metastasis (TNM) grading system.²⁶ All patients were followed up to monitor any postoperative complications after gastrectomy. All patients provided written informed consent, and the Ethical Committee of PKUCH approved this study.

Data collection

The sex, age, tumor size, tumor location, Lauren's classification, TNM classification, surgical setting, duration of surgery,

blood loss, internal to first aerofluxus and postoperative complications of enrolled patients were collected from medical records. Clavien-Dindo classification was used to evaluate postoperative complications.²⁷ Postoperative complications and feasibility were continuously monitored.

Tumor regression grade (TRG) assessment

The NCCN guidelines were used to grade tumor regression for neoadjuvant treatment in patients with AGC,²⁶ as follows: Grade 0, complete regression with no residual tumor cells; Grade 1, near-complete response with single cells or rare small groups of cancer cells; Grade 2, partial tumor regression, with residual cancer cells with evident tumor regression, but more than single cells or rare small groups of cancer cells; and Grade 3, extensive residual cancer with no evident tumor regression. TRG 0 was defined as pCR. The major pathological response (MPR) was defined as the sum of the complete regression and near-complete response. Patients with TRG 0–1 were defined as responders, while non-responders with TRG 3.

Identification of molecular subtypes

DNA mismatch repair (MMR) was evaluated by immunohistochemical analysis of four key proteins, *viz.* MLH-1, MSH-2, MSH-6, and PSM2. Any loss of the above four proteins was defined as MMR deficiency (dMMR); otherwise defined as proficient MMR (pMMR). Epstein-Barr virus (EBV) status was identified by examination of EBV-encoded small RNA (EBER) *in situ* hybridization according to the standard protocol.²⁸

Histological assessment and identification of histopathological immune phenotypes of residual viable tumors

Hematoxylin & Eosin (H&E)-stained slides from the primary tumors were provided by the Pathology Department of our hospital, and the histological assessment was performed by at least two pathologists based on previous literature.²⁹

The percentage of RVT was calculated using the following formula:²⁹

$$\%RVT = \frac{\text{sum of viable tumor area}}{\text{total tumor bed area (viable tumor + regression bed + necrosis)}} \times 100\%.$$

Immunohistochemistry (IHC)

IHC experiments were performed to evaluate immune cell proportions in cancer nests. Fifteen paraffin-embedded AGC patients' cancer tissues following PD-1 blockade plus chemotherapy (15 responders and 5 non-responders) were cut into 5-um thick slices for IHC analysis. Antigen retrieval was performed using antigen repair buffer under high pressure and high-temperature conditions. After that, these slices were blocked with goat serum for 40 min at 37°C and then followed by incubation with the anti-CD4 antibody (ab133616, Abcam), anti-CD8 antibody (ab237710, Abcam) and anti-CD68 antibody (ab955, Abcam) at 4°C for 12 hours. This was followed by three washes with PBS for 5 min and incubation with

secondary antibodies (Dako, Shanghai, China) at 37°C for 40 min. Then, the *DAB* staining was performed using a *DAB* Detection Kit (Dako). After that, 10% hematoxylin was used for Counterstaining before counting the number of positive cells. The number was counted in 6 tumor nest areas at a high-power field (400×), and the average number was used.

Multiplex immunofluorescence (mIF)

Multiplex immunofluorescence staining was conducted using the Akoya OPAL Polaris 7-Color Automation IHC kit (NEL871001KT). FFPE tissue slides were first deparaffinized in a BOND RX system (Leica Biosystems) and then incubated sequentially with primary antibodies targeting CD3 (1:1, Dako, A0452), CD4 (1:100: Abcam, ab133616), CD8 (1:200, Abcam, ab178089), CD56 (1:1000, Abcam, ab75813), CD163 (1:500, Abcam, ab182422), CD68 (1:1000, Abcam, ab213363), PD-1 (1:200, CST, D4W2J, 86163S), PD-L1 (1:400, CST, E1L3N, 13684S), CD20 (1:1, Dako, L26, IR604), FOXP3 (1:100, Abcam, ab20034) and pan-CK (1:100, Abcam, ab7753) (Akoya Biosciences). After that, these slides were incubated with secondary antibodies and corresponding reactive Opal fluorophores. DAPI was used to stain nuclei acids. Tissue slides that have been bound with primary and secondary antibodies but not fluorophores were then included as negative controls to assess autofluorescence. A Vectra Polaris Quantitative Pathology Imaging System (Akoya Biosciences) was used to scan multiplex stained slides at 20 nm wavelength intervals from 440 nm to 780 nm. Then, the complete image for each slide was created by superimposing all scans. Multilayer images were imported to inForm v.2.4.8 (Akoya Biosciences) for quantitative image analysis. Tumor tissues and stromal tissues were differentiated by Pan-CK staining. The quantities of various cell populations were expressed as the number of stained cells per square millimeter and as the percentage of positively stained cells in all nucleated cells.

Cell culture

The MFC gastric cancer cell line was derived from 615-mouse and obtained from the Shanghai cell bank, Chinese Academy of Sciences. The cells were then incubated in DMEM containing 10% fetal bovine serum (FBS, Invitrogen, Carlsbad, CA, USA) and 1% penicillin/streptomycin (Invitrogen), and cultured at 37°C with 5% CO₂.

Animal models

Female 615 mice (5–6 weeks) obtained from Hengrong Biotechnology Co., LTD (Jinan, Shandong, China) were raised under Specific-pathogen-free (SPF) conditions. The animal Care and Use Committee of Peking University Cancer Hospital approved all animal experimentation before implementation. For subcutaneous transplantation, 1 × 10⁵ MFC cells were subcutaneously injected into the back of the right forelimb. After that, the volume of xenograft tumor and body weight were measured at two-day intervals. Nine days after

transplantation, the tumor nodules were palpable, and then the mice were intraperitoneally injected with chemotherapeutic agents (5-fluorouracil at 30 mg/kg and oxaliplatin at 5 mg/kg), or PD-1 antibody (Bio X cell, 10 mg/kg), or combinational therapy of the above drugs once every three days. The tumor volume was calculated as follows: length × width² × 0.5. After three cycles of treatment, the mice were sacrificed by cervical dislocation and tumor samples were collected.

Multiple color flow cytometry

Tumor tissues were minced into 2 × 2 × 2 mm³ pieces by scissors and then treated in a solution comprised of 95% RPMI 1640, 2% FBS, 1% collagenase IV solution, 1% DNase I, and 1% Dispase II for 25 min. After that, the single cells were collected by centrifugation (4000 rpm/5 min) and filtered using the 40-μm filter. Filtered single cells were incubated with anti-mouse CD45, CD4, CD8, CD11b, CD68, CD44, CD62L, 7-AAD, CD274 (PD-L1), CD279 (PD-1), CD206, Gr-1, TNF-α and F4/80 (BioLegend and BD Biosciences) respectively according to the manufacturer's instruction. A BD FACS flow cytometer (FACSCelesta SORP) was used to detect and analyze the data.

Clinical assessment

We collected CT images at baseline and preoperative. At least two radiologists performed imaging assessments based on the RECIST criteria version 1.1.³⁰ In brief, we defined the responses as follows: complete response (CR), the disappearance of all target lesions; partial response (PR), at least a 30% decrease in the sum of diameters of target lesions than that at baseline; progressive disease (PD), at least 20% increase (at least 5 mm) in the sum of diameters of target lesions than the smallest sum in the study, along with the appearance of new lesions; and stable disease (SD), situations between PR and PD. The ORR was defined as the sum of CR and PR.

Statistical analysis

The data are presented as the median and percentage of patients who experienced pCR. The relationship between pathological responses and clinicopathological characteristics was assessed using U-test and chi-square test. RNA expression data of responders and non-responders to PD-1 blockade were obtained from the European Nucleotide Archive under accession PRJEB25780. R 'limma' package was used to identify differentially expressed genes and KEGG enrichment was performed based on the kobas website (<http://kobas.cbi.pku.edu.cn/genelist/>). Based on the global gene expression of patients, the proportion of 22-type infiltrating immune cells in each tumor were calculated using the cibersortx software (<https://cibersortx.stanford.edu>).³¹ Statistical significance was set at *P* < .05, and the reported *P* values were two-sided. Statistical analyses were performed using SPSS software version 23 (SPSS for Windows, Inc., Chicago, IL, USA) and GraphPad Prism 8 (GraphPad Software, USA).

Results

Baseline characteristics of patients

Between June 2017 and May 2022, 75 participants with stage III GC were retrospectively included and Table 1 describes the baseline information. This study was mainly performed on male (80.0%) patients with cTNM stage III (100.0%) GC. The median ages were 64 (range: 27–80). The median follow-up duration was 10.0 months. Of these, 59 (78.7%) patients were pMMR; 14 patients (18.7%) were dMMR and 2 patients without correlated data. In addition, 10 (13.3%) patients were HER2-positive.

Neoadjuvant treatment and tumor pathological regression

All 75 patients with stage III GC underwent neoadjuvant PD-1 blockade plus chemotherapy prior to surgery, and then received D2 gastrectomy. The regimens of neoadjuvant chemotherapy were 5-fluorouracil-based, including SOX (69.3%, 52/75), XELOX (20.0%, 15/75) and others (10.6%, 8/75); while the PD-1 blockade was achieved by PD-1 antibodies (100%, 75/75). The median number of neoadjuvant therapy cycles was 4 and 72 (96%) patients received initially planned 2–6 cycles. Besides, 8 (80%) of 10 patients with HER2-positive received additional treatment with Herceptin (anti-HER2). After surgery, resected specimens underwent pathological evaluation by two pathologists according to the NCCN guidelines.

A total of 21 patients (28.0%) with cTNM-stage III GC achieved pCR in the primary tumor and lymph nodes and only 13 patients showed non-response to this treatment

Table 1. Baseline clinical characteristics.

Characteristic	No. of patients (%)
Total number	75 (100.0)
Gender	
Male	60 (80.0)
Female	15 (20.0)
Median age (range)	64 (27–80)
Tumor location	
Gastroesophageal junction	21 (28.0)
Upper gastric	18 (24.0)
Middle gastric	7 (9.3)
Lower gastric	29 (38.7)
Histological type	
Intestinal	43 (57.3)
Diffuse	15 (20.0)
Mixed	12 (16.0)
Unknown	5 (6.7)
MMR	
dMMR	14 (18.7)
pMMR	59 (78.7)
Unknown	2 (2.7)
HER2	
Positive	10 (13.3)
Negative	57 (76.0)
Unknown	8 (10.7)
cTNM stage	
III	75 (100.0)
CPS	
≤1	12 (16.0)
>1	46 (61.3)
Unknown	17 (22.7)

(Figure 1a). The postneoadjuvant TNM (ypTNM) stage and TRG are summarized in Table 2. Promisingly, 57 (76.0%) patients had a post-therapy pathological downstaging with a ypTNM 0-II stage. Besides, we also calculated the proportion of RVT and tumor necrosis, and the results showed that 60 patients had tumor necrosis more than 50% (Figure 1b). The above results demonstrated that PD-1 blockade plus chemotherapy could induce more intense pathological responses, cause more tumor necroses and elevate the pCR rate in patients with stage III GC.

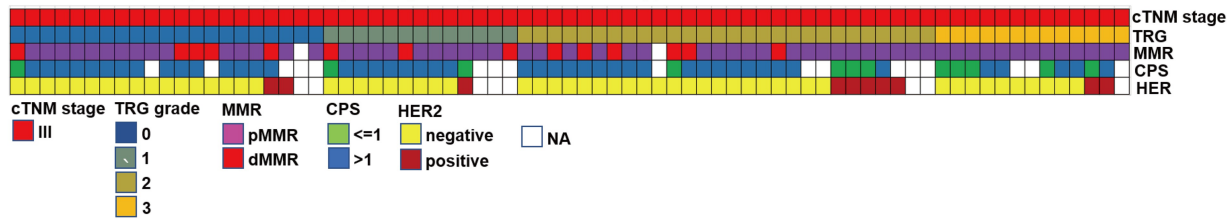
Subgroup analyses

To further investigate the features of patients who achieved pCR, we performed a series of subgroup analyses. Of all enrolled patients, we identified 59 and 14 patients with pMMR and dMMR GC, respectively, while the data for the others were unavailable. In the dMMR subgroup analysis, pCR was achieved in five of 14 (35.7%) patients and 25.4% (15/59) in pMMR (Figure 1c). Furthermore, there were no non-responders in the dMMR group and 13 (22.0%) in the pMMR group. In addition, 6 patients were identified as EBV-positive and two (33.3%) of them achieved pCR (Figure 1c). In addition, CPS were measured in 58 patients and 46 of them had a CPS ≤ 1 with a pCR rate of 8.3% (1/12), and CPS > 1 in 12 patients with a 32.6% (15/46) pCR (Figure 1d). The non-response rates were 41.7% and 10.9% in CPS ≤ 1 and CPS > 1 group respectively. Besides, 10 patients were HER2-positive and 8 of them received additional Herceptin (anti-HER2) treatment. The pCR rates in HER2-negative and HER2-positive patients were 29.8% (17/57) and 20.0% (2/10) respectively (Figure 1e). These results revealed that patients with CPS > 1 and dMMR subtype had a higher rate of pCR and a lower rate of non-response.

More immune infiltration in the resected tumor with major response to neoadjuvant PD-1 blockade plus chemotherapy

Increasing studies have revealed that the immune-cell compositions of TME are associated with the response to cancer treatment.²³ To further investigate the pathological mechanism, we first analyzed the histological features of the tumor nest following neoadjuvant therapy by H&E staining. The results showed that there were substantial infiltrating immune cells in the cancer foci of responders (TRG 1) to neoadjuvant PD-1 blockade plus chemotherapy, while only a few immune cells were observed in the stroma surrounding cancer nest in non-responders with TRG 3 (Figure 2a). The regression bed in imaging evaluated responders was characterized by tumor-infiltrating lymphocytes (TILs), TLS, proliferative fibrosis, plasma cells, neovascularization, infiltrating eosinophils, and neutrophils (Figure 2b). Thus, we predicted that PD-1 blockade plus chemotherapy elevated the efficacy of neoadjuvant therapy by increasing anti-tumor immunity. To verify this prediction, we further analyzed the features of immune cell proportions in TME between responders and non-responders by IHC. The results showed that there was a higher level of

a The information of pathological response grading and several subtypes



b The ratio of tumor necrosis following neoadjuvant PD-1 blockade plus chemotherapy

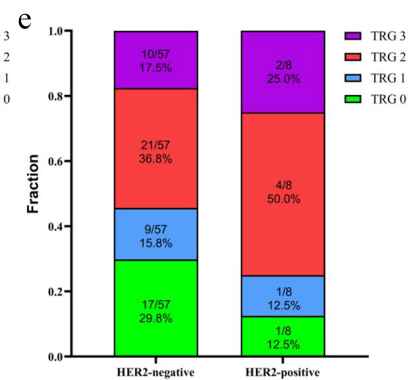
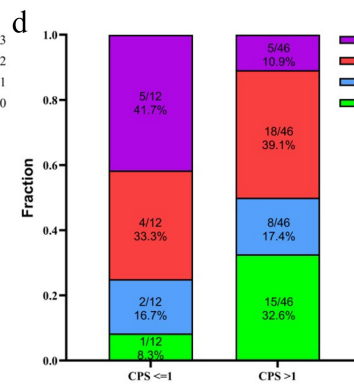
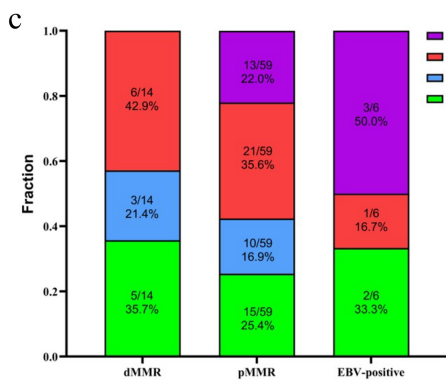
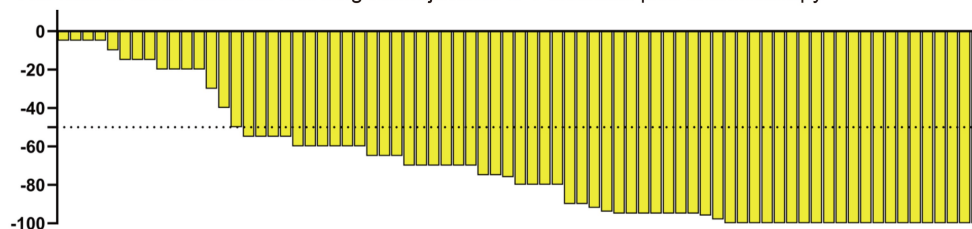


Figure 1. Pathological evaluation to response to neoadjuvant treatment in clinical TNM-stage III gastric cancer (GC) patients. (a) The information of tumor regression grades and several subgroups, including MMR, EBV, CPS and HER2. (b) The ratio of tumor necrosis patients following neoadjuvant PD-1 blockade plus chemotherapy. (c) The tumor regression grades in dMMR, pMMR and EBV-positive patients. (d) The tumor regression grades in CPS ≤ 1 and CPS > 1 patients. (e) The tumor regression grades in HER2-negative and HER2-positive patients.

Table 2. Pathologic Characteristics of Patients.

Characteristic	No. of patients (%)
ypT-category	
0	21 (28.0)
1	9 (12.0)
2	9 (12.0)
3	26 (34.7)
4	10 (13.3)
ypN-category	
0	48 (64.0)
1	10 (13.3)
2	5 (6.7)
3	12 (16.0)
ypTNM-stage	
0	21 (28.0)
1	15 (20.0)
2	21 (28.0)
3	18 (24.0)
TRG	
0	21 (28.0)
1	13 (17.3)
2	28 (37.3)
3	13 (17.3)

immune cell filtration, such as CD8 T cell and CD68 macrophage, in the residual tumor nests of responders, compared to non-responders (Figure 2c).

More infiltrated CD8 + T cells, plasma cells and higher M1/M2 macrophage ratio were associated with the response to neoadjuvant PD-1 blockade plus chemotherapy

To further analyze the factors related to treatment response, we performed a comprehensive analysis based on the RNA expression profile from 12 responders (CR/PR) and 33 non-responders (SD/PD) to PD-1 blockade treatment for GC in Samsung Medical Center.²⁰ Using the R 'limma' package, a total of 1,122 up-regulated (FC > 1.5, p < .05) and 252 down-regulated (FC < 0.67, p < .05) genes in the non-responders were identified (Figure 3a). Of them, several immune suppressive checkpoints, including PDCD1 (PD-1), CD274 (PD-L1), LAG3 and HAVCR2 (TIM-3), were significantly higher in the responders (Figure 3b) and this result was consistent with CPS>1 patient had a higher rate of pCR. To further understand the function of these differentially expressed genes, we performed KEGG analysis and the results found that many immune-related signaling pathways were identified in the top 20, such as PI3K-Akt, TGF-beta, inflammatory mediator regulation of TRP channels and PD-L1 expression and PD-1 checkpoint in cancer (Figure 3c). Then, 22-type infiltrating immune cells were analyzed using the cibersortx software

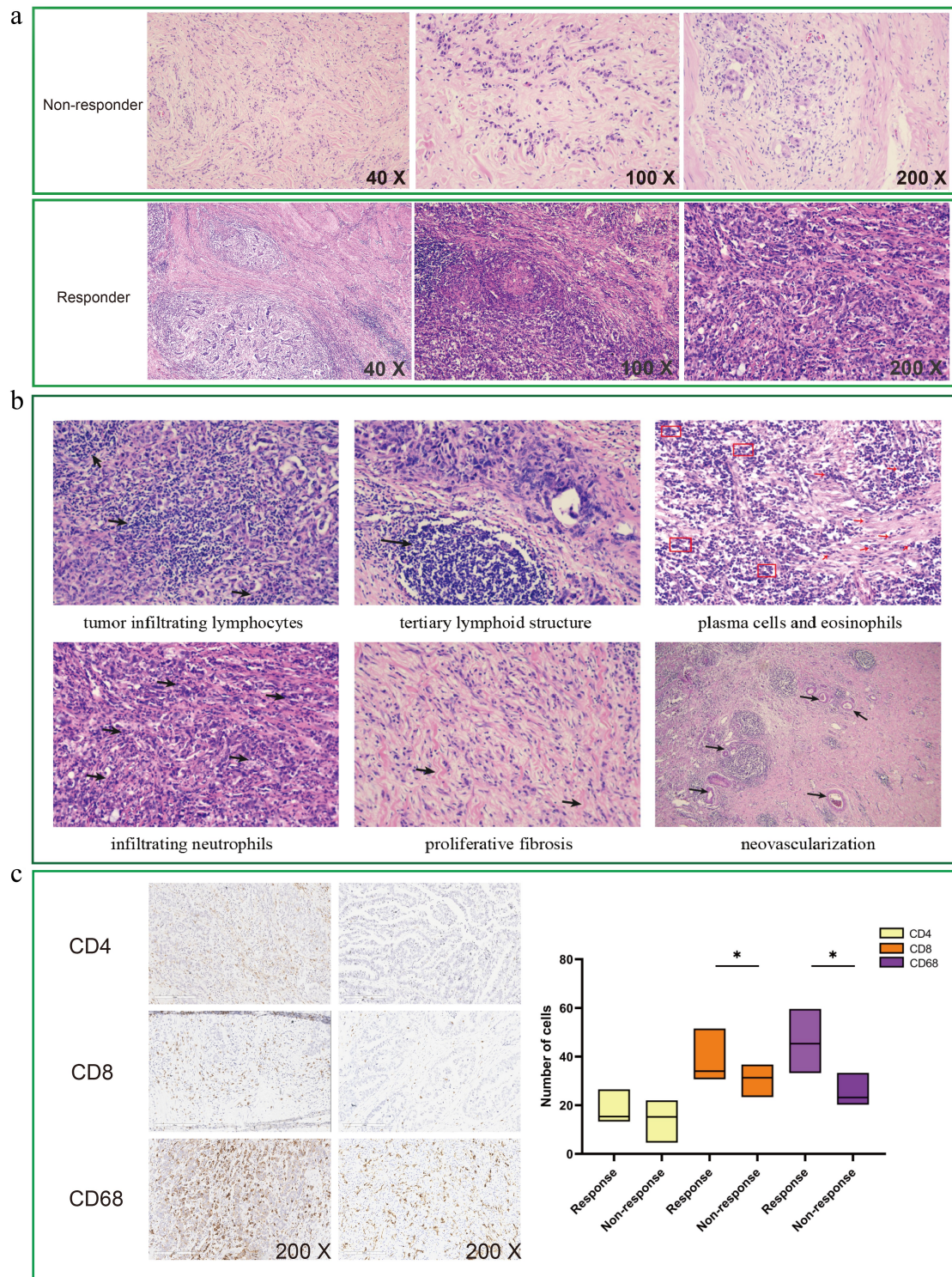


Figure 2. Histological features of cancer foci following different neoadjuvant PD-1 blockade plus chemotherapy. (a) Hematoxylin and eosin (H&E) results observed substantial tumor-infiltrating immune cells in the tumor nests of responders to neoadjuvant PD-1 blockade plus chemotherapy, while rare in the non-responder group. (b) The histopathological features in resected specimens: presence of abundant infiltrating immune cells (tumor infiltrating lymphocytes, plasma cells, eosinophils and neutrophils), tertiary lymphoid structure (TLS), proliferative fibrosis and neovascularization in the regression bed. (c) Immunohistochemistry (IHC) results showed that responders to neoadjuvant treatment had higher levels of CD8⁺ T cells and CD68⁺ macrophages, compared to non-responders.

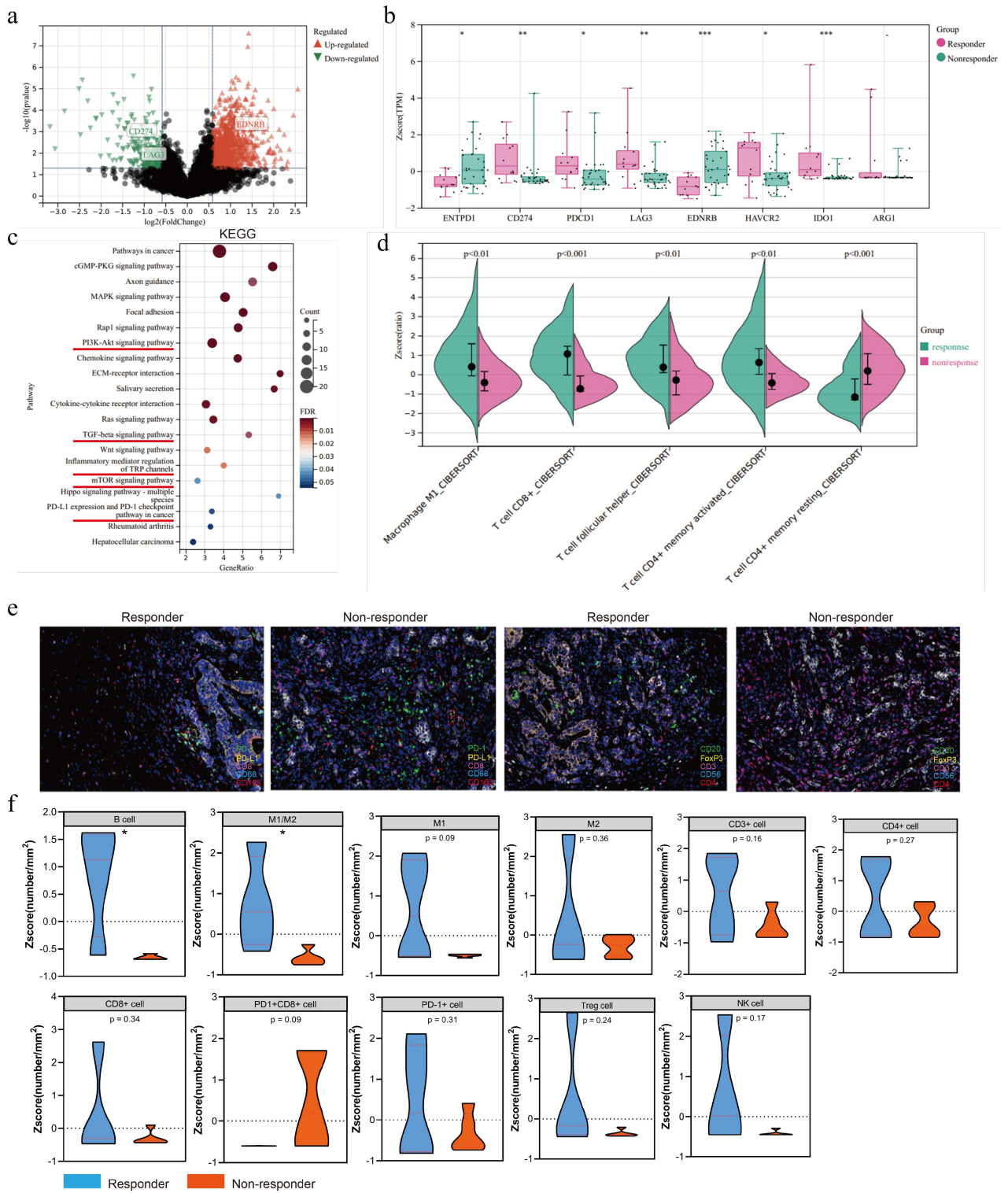


Figure 3. Tumor microenvironment features of immune cells in responders and non-responders to PD-1 blockade. (a) Volcano plots of differentially expressed genes between non-responders and responders to PD-1 blockade. (b) Immune suppressive checkpoints between non-responders and responders to PD-1 blockade. (c) The top 20 enriched KEGG pathways of the differentially expressed genes. (d) Differentially infiltrated immune cells, identified by the CIBERSORT method, between non-responders and responders to PD-1 blockade. (e) Multicolor immunofluorescence in one representative responder and one non-responder treated with neoadjuvant PD-1 blockade plus chemotherapy. (f) The proportions of immune cells identified by multicolor immunofluorescence in 4 responders and 5 non-responders to neoadjuvant PD-1 blockade plus chemotherapy.

(<https://cibersortx.stanford.edu>).³¹ Consistent with the above results, M1-type macrophage, CD8 + T cell and CD4+ memory-activated T cell were up-regulated in the responders.

To verify this, we further performed mIF experiments between 4 responders (TRG 1) and 5 non-responders (TRG 3) from our cohort (Figure 3d). The results showed that an increased immune signature and high immune infiltration were observed in the residual tumor nests of responders compared to non-responders. There were increased B cells ($p < .05$), CD4 + T cells ($p = .27$), CD8 + T cells ($p = .34$), M1-macrophage ($p = .09$) and elevated M1/M2-macrophage ratio ($p = .05$) in the TME of responders (Figure 3e). Furthermore, PD-1⁺CD8⁺ T lymphocytes were only observed in the residual viable tumor of non-responders ($P = .079$, Figure 3e). All these results indicated that more infiltrated CD8 + T cells, plasma cells and higher M1/M2 macrophage ratio in the tumor nests were associated with the response to neoadjuvant PD-1 blockade plus chemotherapy.

A combination of PD-1 blockade plus chemotherapy inhibits tumor growth more pronounced compared to chemotherapy in vivo

To further confirm the roles of PD-1 blockade and chemotherapy in neoadjuvant therapy in AGC, we applied four strategies in MFC tumor-bearing 615-mice, including control (PBS), chemotherapy, anti-PD-1 antibody treatment or PD-1 blockade plus chemotherapy (Figure 4a). Five mice were used in each group. After 2-cycle treatment, the mice were sacrificed to analyze the changes in immune cell proportion and the tumors were resected. More significant regression in tumor size was observed in the PD-1 blockade plus chemotherapy group ($P < .05$, Figure 4b), while all experimental mice showed no significant weight loss. To further verify the effects of the above treatments on GC, we performed the experiments with longer periods of observation. We monitored the tumor volumes and observed smaller volumes in the PD-1 blockade and PD-1 blockade plus chemotherapy group, compared to the control ($P < .01$, Figure 4c-d). Furthermore, a significant advantage of PD-1 blockade and PD-1 blockade plus chemotherapy was also observed when compared to chemotherapy ($P < .05$, Figure 4c-d).

PD-1 blockade plus chemotherapy induced more CD8 + T cells and elevated M1/M2 ratio in a mouse model

We further investigated the effects of the above treatments on immune cell populations of the spleen, which reflects the systemic immune function and involves in nonspecific and specific immunity.³² The results showed that PD-1 block plus chemotherapy (5-fluorouracil and oxaliplatin) significantly increased the levels of CD8⁺ CD44⁺CD62L⁻ effector T cells, compared to chemotherapy alone (Figure 4e,f, $p < .05$). In addition, TNF- α is an important cytokine by which CD8⁺ T cells exert anti-tumor effects.³³ A higher level of TNF- α was also found in the CD8⁺ T cells following PD-1 blockade plus chemotherapy compared to only chemotherapy (Figure 4g, $p = .057$). These results suggested that PD-1 block

plus chemotherapy enhanced the anti-tumor functions of CD8⁺ T cells in vivo.

Recent studies also revealed that tumor-associated macrophages play an important role in cancer progression. We then assessed the effects of the above therapeutic strategies on macrophages in this study. The results showed that PD-1 block plus chemotherapy decreased the number of total macrophages (CD11b⁺F4/80⁺) (Figure 5a, b), but elevated the ratio of M1(CD11b⁺F4/80⁺ CD206⁻)/M2(CD11b⁺F4/80⁺CD206⁺) (Figure 5c-e). Furthermore, in the adjacent and cancerous tissues of one patient with major tumor regression and clinically evaluated partial response (figure 5f), abundant infiltrated CD8 + T cells and M1 macrophages were detected (Figure 5g). These results suggested that PD-1 block plus chemotherapy induced synergistic effects for recruiting anti-tumor immune subsets and achieved a better therapeutic efficacy compared to only chemotherapy.

Safety and feasibility

Detailed information regarding surgery is also presented in Table 3. The interval between the last neoadjuvant therapy and surgery was 3–5 weeks. There were 54.7% (41/75) and 45.3% (34/75) patients who received total and subtotal gastrectomy respectively, and the R0 resection rate was 98.7% (74/75). The average duration of operation and median blood loss were 4.02 h and 100.0 mL respectively. The median time interval from surgery to the first aerofluxus was 4.0 days. Neoadjuvant PD-1 blockade did not influence the difficulty level to perform gastrectomy and the recovery of gastrointestinal function.

In addition, Table 3 also lists information on postoperative complications and no previously unreported postoperative complications occurred in the present study. In brief, complications following surgery occurred in 22 (29.3%) patients with stage III GC who received neoadjuvant PD-1 blockade plus chemotherapy. Abdominal infection (7/75, 9.4%) and pulmonary infection (5/75, 6.7%) were the most prevalent postoperative complications. There were 4 (5.3%) serious complications (CD grade 3 or higher), including 2 abdominal infections, 1 pulmonary infection and 1 anastomotic bleeding. Furthermore, all postoperative complications were under control and they caused no death. These results indicated that patients with neoadjuvant PD-1 blockade plus chemotherapy did not increase the rate of serious complications.

Discussion

Considering the significant survival benefit achieved by first-line PD-1 blockade and chemotherapy (5-fluorouracil and oxaliplatin) in GC, data on neoadjuvant treatment are important and expected.¹⁸ Herein, we firstly reported that neoadjuvant PD-1 blockade plus chemotherapy led to a pCR rate of 28.0% in patients with cTNM-stage III GC. The pCR rate due to treatment with neoadjuvant PD-1 blockade plus chemotherapy was significantly higher than the 4.6%-10% in traditional neoadjuvant chemotherapy.^{7,8} Furthermore, fewer patients had no significant response to treatment.

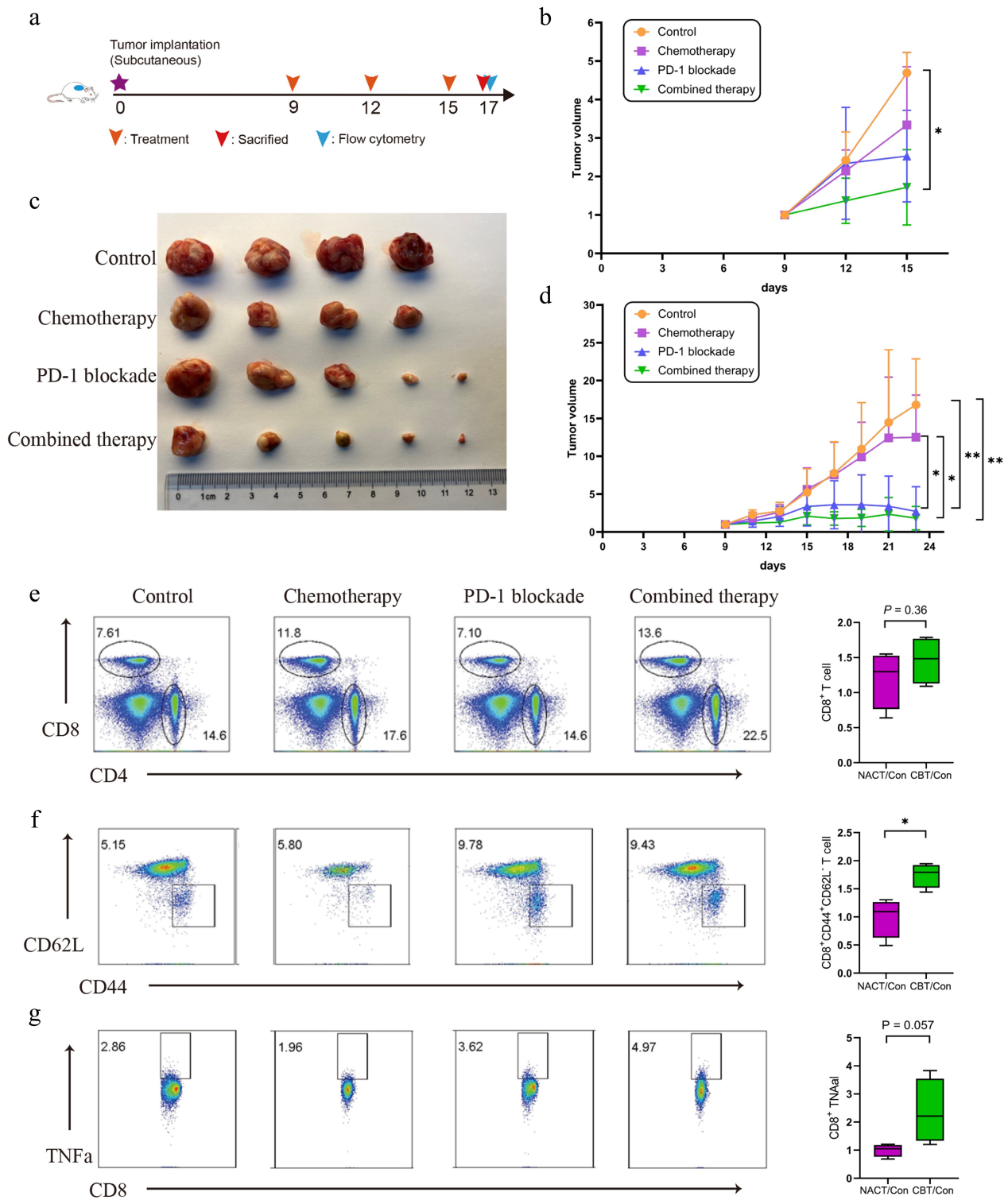


Figure 4. PD-1 blockade plus chemotherapy inhibits tumor growth by inducing more anti-tumor immune subsets in mouse models. (a) Treatment protocol for PD-1 inhibitor and chemotherapy in 615-mice. At the end, tumors were collected and analyzed by multi-color flow cytometry. (b) The tumor sizes of 615 mice treated with chemotherapy (5-fluorouracil and oxaliplatin) and/or PD-1 inhibitor before flow cytometry. (c-d) The changes of tumor volumes of 615 mice treated with the four strategies in a longer period of observation. Staining of CD4⁺ T cells (e), CD8⁺ T cells (E), effector CD8⁺CD44⁺CD62L⁺ T cells (f) and intracellular cytokine staining of TNF- α CD8⁺ T cells (g) among CD45⁺ T cells.

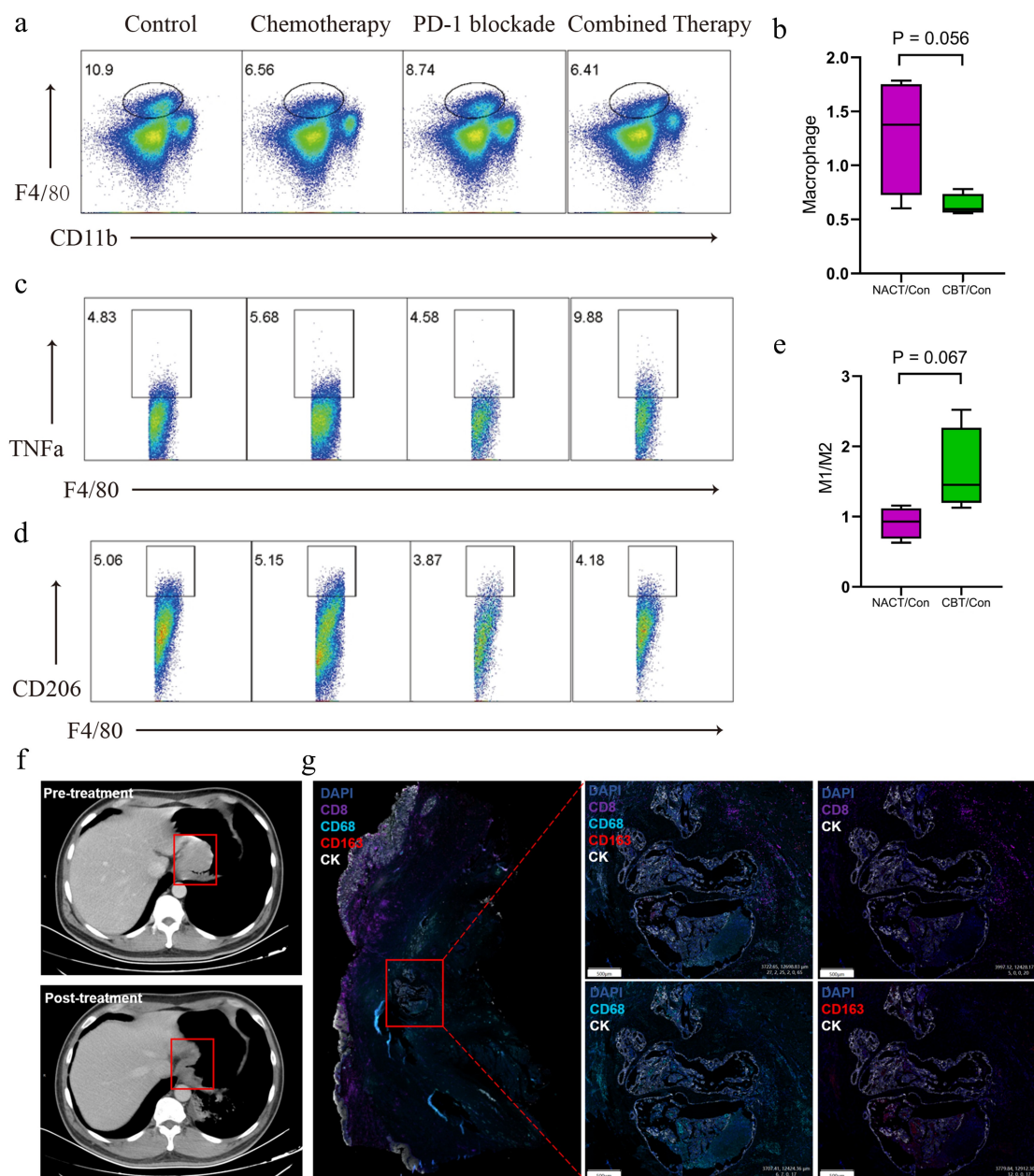


Figure 5. PD-1 blockade and chemotherapy regulated macrophages to inhibit tumor progression in mouse models. (a-b) Chemotherapy (5-fluorouracil and oxaliplatin) and PD-1 inhibitor decreased macrophages and exerted synergic effects in combinational group. (c-e) Combining PD-1 blockade and chemotherapy could increase M1-type macrophages and decreased M2-type macrophages to elevate the ratio of M1/M2. (f) The CT images at pre- and post-PD-1 blockade plus chemotherapy of one case with clinically evaluated partial response. (g) The proportions of CD8⁺ T cells and macrophages identified by multicolor immunofluorescence in the above case. CBT: PD-1 blockade plus chemotherapy.

The specific mechanism by which chemo-immunotherapy exerts its effects is not clear. Although several studies revealed that chemotherapy induces antitumor immune subsets and exerts synergic effects with immune checkpoint inhibitors in cancer treatment,^{25,34} inconsistent results were also found.²³ Therefore, it is highly necessary to investigate the treatment efficacy of neoadjuvant PD-1 blockade plus chemotherapy in GC patients and explore the specific mechanisms. We investigated the cell types and histological structures of cancer nests following neoadjuvant PD-1 plus chemotherapy and uncovered the histological features associated with therapeutic strategies and responses. Our analyses indicated that the cancer foci of patients who received neoadjuvant PD-1 blockade plus

chemotherapy and achieved major response were characterized by substantial infiltrating immune cells, while rare immune cells were observed in the non-response group. To confirm the effects of increased immune infiltration, we further analyzed the immune features in the residual viable tumor of responders and non-responders and a higher proportion of antitumor immune cell subsets was also observed in responders.

TME has been proven to be an integral part of tumor²² and the TME compositions significantly influence the tumor progression and responses to treatment, especially T cells and tumor-associated macrophages.²⁴ It is commonly accepted that CD8⁺ T lymphocytes and M1-type macrophages play an antitumor role

Table 3. Detailed information regarding surgery and postoperative complications.

Characteristic	No. of patients (%)	
Surgery	75	
Mode		
Total gastrectomy	41 (54.7)	
Subtotal gastrectomy	34 (45.3)	
Surgical time (average, h)	4.02	
R0 resection (percent)	74 (98.7)	
Bleeding (median, mL)	100	
Resected lymph nodes	2 (20 ~ 83)	
Median number (range)		
First aerofluxus (median, days)	4	
Postoperative complications	Grade 1–2	Grade 3 or higher
Any	18 (24.0)	4 (5.3)
Abdominal infection	5 (6.7)	2 (2.7)
Pulmonary infection	4 (5.3)	1 (1.3)
Anastomotic bleeding	-	1 (1.3)
Incision infection	1 (1.3)	-
Anastomotic leak	1 (1.3)	-
Pleural fluid	1 (1.3)	-
Myocardial ischemia	2 (2.7)	-
Atrial tachycardia	1 (1.3)	-
Chylous fistula	1 (1.3)	-
Adynamic intestinal obstruction	1 (1.3)	-
Anastomotic stenosis	1 (1.3)	-

and M2-type macrophages exert protumor effects. Exploring the associations between immune cell proportions in TME and clinical outcomes contribute to understanding the evolution of tumor following treatment and analyzing the optimum therapeutic regimen. We then analyze the immune features on samples following PD-1 blockade plus chemotherapy of cTNM-stage III GC patients with or without response. The results showed that responders had a higher level of immune infiltration, such as a higher M1/M2 macrophage ratio and increased B cells.

To further verified the enhanced anti-tumor effects of PD-1 blockade plus chemotherapy on GC, animal experiments were performed on 615-mice and 615-mouse-derived GC cell line (MFC). Our analyses in the mouse models revealed that PD-1 blockade plus chemotherapy could effectively inhibit tumor growth and elevate the levels of effector (CD8⁺CD44⁺CD62L⁻) T cells and M1/M2 ratio of macrophages, compared to chemotherapy alone.

Although a significant elevation of pCR was achieved in the combinational therapy group, several patients remain non-response (13/75, 17.3%) to treatment. Thus, identifying the sensitive subpopulation is a key issue for further improving clinical outcomes, but no validated molecular markers have yet been well established. Commonly used clinical indicators for immunotherapy included CPS, MSI-H/dMMR and EBV status.^{12,35–37} However, an all-inclusive comprehensive clinical study remains vacant. Then, we performed a series of subgroup analyses and found that patients with CPS>1, dMMR and EBV-positive had a higher rate of pCR. In addition, additional Herceptin (anti-HER2) treatment can not increase the pCR rate in patients with HER2-positive cTNM-stage III GC treated by neoadjuvant PD-1 blockade plus chemotherapy. However, patients with pMMR also achieved a 25.4% pCR rate, significantly higher than traditional neoadjuvant chemotherapy. In summary, neoadjuvant PD-1 blockade plus chemotherapy achieved significantly better efficacy in all subgroups and should be more prevalence in clinical treatment for cTNM-stage III GC.

Despite encouraging efficacy, the safety of the combinational treatment strategy is worrisome. Previous studies have reported mild and easily controllable toxicity and side effects of PD-1 blockade plus chemotherapy in GC.^{18,38} We analyzed the surgery-related information, rates of postoperative complications and serious events. The results demonstrated that additional PD-1 blockade did not increase the difficulty of surgery. Besides, no significant increase in serious events of postoperative complications. Therefore, these results suggest that preoperative PD-1 blockade plus chemotherapy is a safe, feasible, and promising therapeutic strategy for patients with cTNM-stage III GC.

Of course, there were several limitations in our study. First, this study employed a single-center design, which may have compromised the results. Therefore, multi-center studies are needed to validate our findings. Second, although more intense immune infiltration and survival benefit were found in the PD-1 blockade plus chemotherapy group, the underlying molecular mechanisms behind these phenomena remained unclear. Besides, further efforts are warranted to explore potential biomarkers related to therapeutic efficacy.

Conclusion

The present study showed that neoadjuvant PD-1 blockade plus chemotherapy can achieve a promising pCR rate in patients with cTNM-stage III GC. Patients characterized with CPS>1 and dMMR may be more sensitive to neoadjuvant PD-1 blockade plus chemotherapy. More infiltrated plasma cells, CD8⁺ T cells and elevated M1/M2 macrophage ratio are associated with a better response to neoadjuvant PD-1 blockade plus chemotherapy. In addition, PD-1 blockade plus chemotherapy could induce more infiltrated anti-tumor immune cell subpopulations, including CD8⁺CD44⁺CD62L⁻ effector T cells and M1-polarized macrophages, to achieve better efficacy compared to chemotherapy alone. Furthermore, neoadjuvant PD-1 blockade plus chemotherapy neither delayed surgery nor increased postoperative complication rate. These results indicate neoadjuvant PD-1 blockade plus chemotherapy is a promising therapeutic strategy in patients with cTNM-stage III GC.

Disclosure statement

The authors declare that they have no competing interests.

Funding

This study was funded by National Natural Foundation of China (82272655, 31870805), Joint Funds of the Hospital Management Center in Beijing (QML20201104), National Natural Science Foundation of China (U20A20371), Innovation Fund for Excellent Ph.D. students of Peking University Health Science Center (2011110636) and Chinese Society of Clinical Oncology (Y-HR2019-0375).

ORCID

Ziyu Li  <http://orcid.org/0000-0001-5580-4979>

Author contributions

GXY and LZY had full access to all the data in this present study and provided the guidance throughout the preparation of this manuscript. TXH and LMY contributed equally to this study. Concept and design: TXH, GXY and LZY. Collection and analysis of the data: all authors. Drafting of the manuscript: TXH, GXY and LZY. Statistical analysis: WXL, ZY, HY, WZ and JFZ. Radiological and pathological analysis: SF, TL, LJ and ZL. Animal experiments: LMY, TXH, GT and XXF. Obtained funding: GXY and LZY. Supervision: GXY and LZY.

Data availability statement

The RNA expression profile of GC patients treated by PD-1 blockade in Samsung Medical Center was downloaded from the European Nucleotide Archive (PRJEB25780). The original data presented in this study are included in the article or supplement materials, other information can be directed to the corresponding authors.

References

- Sung H, Ferlay J, Siegel RL, Laversanne M, Soerjomataram I, Jemal A, Bray F. Global cancer statistics 2020: GLOBOCAN estimates of incidence and mortality worldwide for 36 cancers in 185 countries. *CA Cancer J Clin.* 2021;71(3):209–249. doi:10.3322/caac.21660.
- Cunningham D, Allum WH, Stenning SP, Thompson JN, Van de Velde CJ, Nicolson M, Scarffe JH, Lofts FJ, Falk SJ, Iveson TJ, et al. Perioperative chemotherapy versus surgery alone for resectable gastroesophageal cancer. *N Engl J Med.* 2006;355(1):11–20. doi:10.1056/NEJMoa055531.
- Al-Batran SE, Homann N, Pauligk C, Goetze TO, Meiler J, Kasper S, Kopp HG, Mayer F, Haag GM, Luley K, et al. Perioperative chemotherapy with fluorouracil plus leucovorin, oxaliplatin, and docetaxel versus fluorouracil or capecitabine plus cisplatin and epirubicin for locally advanced, resectable gastric or gastro-oesophageal junction adenocarcinoma (FLOT4): a randomised, phase 2/3 trial. *Lancet.* 2019;393(10184):1948–1957. doi:10.1016/S0140-6736(18)32557-1.
- Yang L, Ying X, Liu S, Lyu G, Xu Z, Zhang X, Li H, Li Q, Wang N, Ji J. Gastric cancer: epidemiology, risk factors and prevention strategies. *Chin J Cancer Res.* 2020;32(6):695–704. doi:10.21147/j.1000-9604.2020.06.03.
- Ajani JA, D'Amico TA, Almhanna K, Bentrem DJ, Chao J, Das P, Denlinger CS, Fanta P, Farjah F, Fuchs CS, et al. Gastric cancer, Version 3.2016, NCCN clinical practice guidelines in oncology. *J Natl Compr Canc Netw.* 2016;14(10):1286–1312. doi:10.6004/jnccn.2016.0137.
- Ychou M, Boige V, Pignon JP, Conroy T, Bouche O, Lebreton G, Ducourtieux M, Bedenne L, Fabre JM, Saint-Aubert B, et al. Perioperative chemotherapy compared with surgery alone for resectable gastroesophageal adenocarcinoma: an FNCLCC and FFCO multicenter phase III trial. *J Clin Oncol.* 2011;29(13):1715–1721. doi:10.1200/JCO.2010.33.0597.
- Schneider BJ, Shah MA, Klute K, Ocean A, Popa E, Altorki N, Lieberman M, Schreiner A, Yantiss R, Christos PJ, et al. Phase I study of epigenetic priming with azacitidine prior to standard neoadjuvant chemotherapy for patients with resectable gastric and esophageal adenocarcinoma: evidence of tumor hypomethylation as an indicator of major histopathologic response. *Clin Cancer Res.* 2017;23(11):2673–2680. doi:10.1158/1078-0432.CCR-16-1896.
- Pereira MA, Ramos M, Dias AR, Cardili L, Ribeiro RRE, Charruf AZ, de Castria TB, Zilberstein B, Ceconello I, Avancini Ferreira Alves V, et al. Lymph node regression after neoadjuvant chemotherapy: a predictor of survival in gastric cancer. *J Surg Oncol.* 2020;121(5):795–803. doi:10.1002/jso.25785.
- Topalian SL, Taube JM, Pardoll DM. Neoadjuvant checkpoint blockade for cancer immunotherapy. *Science.* 2020;367(6477). doi:10.1126/science.aax0182.

- Sasaki A, Nakamura Y, Togashi Y, Kuno H, Hojo H, Kageyama S, Nakamura N, Takashima K, Kadota T, Yoda Y, et al. Enhanced tumor response to radiotherapy after PD-1 blockade in metastatic gastric cancer. *Gastric Cancer.* 2020;23(5):893–903. doi:10.1007/s10120-020-01058-4.
- Blank CU, Rozeman EA, Fanchi LF, Sikorska K, van de Wiel B, Kvistborg P, Krijgsman O, van den Braber M, Philips D, Broeks A, et al. Neoadjuvant versus adjuvant ipilimumab plus nivolumab in macroscopic stage III melanoma. *Nat Med.* 2018;24(11):1655–1661. doi:10.1038/s41591-018-0198-0.
- Chalabi M, Fanchi LF, Dijkstra KK, Van den Berg JG, Aalbers AG, Sikorska K, Lopez-Yurda M, Grootsholten C, Beets GL, Snaebjornsson P, et al. Neoadjuvant immunotherapy leads to pathological responses in MMR-proficient and MMR-deficient early-stage colon cancers. *Nat Med.* 2020;26(4):566–576. doi:10.1038/s41591-020-0805-8.
- Forde PM, Chaft JE, Smith KN, Anagnostou V, Cottrell TR, Hellmann MD, Zahurak M, Yang SC, Jones DR, Broderick S, et al. Neoadjuvant PD-1 blockade in resectable lung cancer. *N Engl J Med.* 2018;378(21):1976–1986. doi:10.1056/NEJMoa1716078.
- Marabelle A, Le DT, Ascierto PA, Di Giacomo AM, De Jesus-Acosta A, Delord JP, Geva R, Gottfried M, Penel N, Hansen AR, et al. Efficacy of pembrolizumab in patients with noncolorectal high microsatellite instability/mismatch repair-deficient cancer: results from the Phase II KEYNOTE-158 study. *J Clin Oncol.* 2020;38(1):1–10. doi:10.1200/JCO.19.02105.
- Moehler M, Shitara K, Garrido M, Salman P, Shen L, Wyrwicz L, Yamaguchi K, Skoczylas T, Bragagnoli AC, Liu T, et al. Nivolumab (nivo) plus chemotherapy (chemo) versus chemo as first-line (1L) treatment for advanced gastric cancer/gastroesophageal junction cancer (GC/GEJC)/esophageal adenocarcinoma (EAC): first results of the CheckMate 649 study. *Ann Oncol.* 2020;31:S1191–S1191. doi:10.1016/j.annonc.2020.08.2296.
- Fuchs CS, Doi T, Jang RW, Muro K, Satoh T, Machado M, Sun W, Jalal SI, Shah MA, Metges JP, et al. Safety and efficacy of pembrolizumab monotherapy in patients with previously treated advanced gastric and gastroesophageal junction cancer: phase 2 clinical KEYNOTE-059 trial. *JAMA Oncol.* 2018;4(5):e180013. doi:10.1001/jamaoncol.2018.0013.
- Shitara K, Van Cutsem E, Bang YJ, Fuchs C, Wyrwicz L, Lee KW, Kudaba I, Garrido M, Chung HC, Lee J, et al. Efficacy and safety of pembrolizumab or pembrolizumab plus chemotherapy vs chemotherapy alone for patients with first-line, advanced gastric cancer: the KEYNOTE-062 Phase 3 randomized clinical trial. *JAMA Oncol.* 2020;6(10):1571–1580. doi:10.1001/jamaoncol.2020.3370.
- Janjigian YY, Shitara K, Moehler M, Garrido M, Salman P, Shen L, Wyrwicz L, Yamaguchi K, Skoczylas T, Campos Bragagnoli A, et al. First-line nivolumab plus chemotherapy versus chemotherapy alone for advanced gastric, gastro-oesophageal junction, and esophageal adenocarcinoma (CheckMate 649): a randomised, open-label, phase 3 trial. *Lancet.* 2021;398(10294):27–40. doi:10.1016/S0140-6736(21)00797-2.
- Gastric Cancer Association CA-CA. Chinese expert consensus on perioperative treatment of locally advanced gastric cancer (2021 version). *Zhonghua Wei Chang Wai Ke Za Zhi.* 2021;24(9):741–748. doi:10.3760/cma.j.cn.441530-20210831-00351.
- Kim ST, Cristescu R, Bass AJ, Kim KM, Odegaard JI, Kim K, Liu XQ, Sher X, Jung H, Lee M, et al. Comprehensive molecular characterization of clinical responses to PD-1 inhibition in metastatic gastric cancer. *Nat Med.* 2018;24(9):1449–1458. doi:10.1038/s41591-018-0101-z.
- Chao J, Fuchs CS, Shitara K, Tabernero J, Muro K, Van Cutsem E, Bang YJ, De Vita F, Landers G, Yen CJ, et al. Assessment of pembrolizumab therapy for the treatment of microsatellite instability-high gastric or gastroesophageal junction cancer among patients in the KEYNOTE-059, KEYNOTE-061, and KEYNOTE-062 clinical trials. *JAMA Oncol.* 2021;7(6):895–902. doi:10.1001/jamaoncol.2021.0275.

22. Pitt JM, Marabelle A, Eggermont A, Soria JC, Kroemer G, Zitvogel L. Targeting the tumor microenvironment: removing obstruction to anticancer immune responses and immunotherapy. *Ann Oncol*. 2016;27(8):1482–1492. doi:10.1093/annonc/mdw168.
23. Zhang Y, Chen H, Mo H, Hu X, Gao R, Zhao Y, Liu B, Niu L, Sun X, Yu X, et al. Single-cell analyses reveal key immune cell subsets associated with response to PD-L1 blockade in triple-negative breast cancer. *Cancer Cell*. 2021;39(12):1578–1593 e1578. doi:10.1016/j.ccell.2021.09.010.
24. Zheng L, Qin S, Si W, Wang A, Xing B, Gao R, Ren X, Wang L, Wu X, Zhang J, et al. Pan-cancer single-cell landscape of tumor-infiltrating T cells. *Science*. 2021;374(6574):abe6474. doi:10.1126/science.abe6474.
25. Kim R, An M, Lee H, Mehta A, Heo YJ, Kim KM, Lee SY, Moon J, Kim ST, Min BH, et al. Early tumor-immune microenvironmental remodeling and response to frontline fluoropyrimidine and platinum chemotherapy in advanced gastric cancer. *Cancer Discov*. 2021;12(4): 984–1001.
26. Sano T, Coit DG, Kim HH, Roviello F, Kassab P, Wittekind C, Yamamoto Y, Ohashi Y. Proposal of a new stage grouping of gastric cancer for TNM classification: international gastric cancer association staging project. *Gastric Cancer*. 2017;20(2):217–225. doi:10.1007/s10120-016-0601-9.
27. Dindo D, Demartines N, Clavien PA. Classification of surgical complications: a new proposal with evaluation in a cohort of 6336 patients and results of a survey. *Ann Surg*. 2004;240(2):205–213. doi:10.1097/01.sla.0000133083.54934.ae.
28. Song HJ, Srivastava A, Lee J, Kim YS, Kim KM, Ki Kang W, Kim M, Kim S, Park CK, Kim S. Host inflammatory response predicts survival of patients with Epstein-Barr virus-associated gastric carcinoma. *Gastroenterology*. 2010;139(1):84–92 e82. doi:10.1053/j.gastro.2010.04.002.
29. Cottrell TR, Thompson ED, Forde PM, Stein JE, Duffield AS, Anagnostou V, Rekhtman N, Anders RA, Cuda JD, Illei PB, et al. Pathologic features of response to neoadjuvant anti-PD-1 in resected non-small-cell lung carcinoma: a proposal for quantitative immune-related pathologic response criteria (irPRC). *Ann Oncol*. 2018;29(8):1853–1860. doi:10.1093/annonc/mdy218.
30. Eisenhauer EA, Therasse P, Bogaerts J, Schwartz LH, Sargent D, Ford R, Dancey J, Arbuck S, Gwyther S, Mooney M, et al. New response evaluation criteria in solid tumours: revised RECIST guideline (version 1.1). *Eur J Cancer*. 2009;45(2):228–247. doi:10.1016/j.ejca.2008.10.026.
31. Newman AM, Steen CB, Liu CL, Gentles AJ, Chaudhuri AA, Scherer F, Khodadoust MS, Esfahani MS, Luca BA, Steiner D, et al. Determining cell type abundance and expression from bulk tissues with digital cytometry. *Nat Biotechnol*. 2019;37(7):773–782. doi:10.1038/s41587-019-0114-2.
32. Lee S, Song IH, Park YS. In vivo and in vitro study of immunostimulation by *Leuconostoc lactis*-produced gluco-oligosaccharides. *Molecules*. 2019;24(21):3994.
33. Osuna-Gomez R, Arqueros C, Galano C, Mulet M, Zamora C, Barnadas A, Vidal S. Effector mechanisms of CD8+ HLA-DR+ T cells in breast cancer patients who respond to neoadjuvant chemotherapy. *Cancers (Basel)*. 2021;13(24):6167. doi:10.3390/cancers13246167.
34. Principe DR, Kamath SD, Korc M, Munshi HG. The immune modifying effects of chemotherapy and advances in chemo-immunotherapy. *Pharmacol Ther*. 2022;236:108111. doi:10.1016/j.pharmthera.2022.108111.
35. Cancer Genome Atlas Research N. Comprehensive molecular characterization of gastric adenocarcinoma. *Nature*. 2014;513(7517):202–209. doi:10.1038/nature13480.
36. Lee V, Murphy A, Le DT, Diaz LA Jr. Mismatch repair deficiency and response to immune checkpoint blockade. *Oncologist*. 2016;21(10):1200–1211. doi:10.1634/theoncologist.2016-0046.
37. Le DT, Uram JN, Wang H, Bartlett BR, Kemberling H, Eyring AD, Skora AD, Luber BS, Azad NS, Laheru D, et al. PD-1 blockade in tumors with mismatch-repair deficiency. *N Engl J Med*. 2015;372(26):2509–2520. doi:10.1056/NEJMoa1500596.
38. Kojima T, Shah MA, Muro K, Francois E, Adenis A, Hsu CH, Doi T, Moriwaki T, Kim SB, Lee SH, et al. Investigators K-. randomized Phase III KEYNOTE-181 study of pembrolizumab versus chemotherapy in advanced esophageal cancer. *J Clin Oncol*. 2020;38(35):4138–4148. doi:10.1200/JCO.20.01888.